Brief Research Report | Genitourinary Imaging

eISSN 2005-8330
https://doi.org/10.3348/kjr.2020.1369
Korean J Radiol 2022;23(1):60-67

Korean Journal of Radiology
KJR

Imaging Patterns of Bacillus Calmette–Guérin-Related Granulomatous Prostatitis Based on Multiparametric MRI

Seungsoo Lee[1], Young Taik Oh[2], Hye Min Kim[3], Dae Chul Jung[2], Hyesuk Hong[4]

[1]Department of Radiology, Research Institute of Radiological Science, Yongin Severance Hospital, Yonsei University College of Medicine, Yongin, Korea; [2]Department of Radiology, Research Institute of Radiological Science, Severance Hospital, Yonsei University College of Medicine, Seoul, Korea; [3]Department of Pathology, Yongin Severance Hospital, Yonsei University College of Medicine, Yongin, Korea; [4]Department of Radiology, Research Institute and Hospital, National Cancer Center, Goyang, Korea

Objective: To categorize multiparametric MRI features of Bacillus Calmette–Guérin (BCG)-related granulomatous prostatitis (GP) and discover potential manifestations for its differential diagnosis from prostate cancer

Materials and Methods: The cases of BCG-related GP in 24 male (mean age ± standard deviation, 66.0 ± 9.4 years; range, 50–88 years) pathologically confirmed between January 2011 and April 2019 were retrospectively reviewed. All patients underwent intravesical BCG therapy followed by a MRI scan. Additional follow-up MRI scans, including diffusion-weighted imaging (DWI), were performed in 19 patients. The BCG-related GP cases were categorized into three: A, B, or C. The lesions with diffusion restriction and homogeneous enhancement were classified as type A. The lesions with diffusion restriction and a poorly enhancing component were classified as type B. A low signal intensity on high b-value DWI (b = 1000 s/mm^2) was considered characteristic of type C. Two radiologists independently interpreted the MRI scans before making a consensus about the types.

Results: The median lesion size was 22 mm with the interquartile range (IQR) of 18–26 mm as measured using the initial MRI scans. The lesion types were A, B, and C in 7, 15, and 2 patients, respectively. Cohen's kappa value for the inter-reader agreement for the interpretation of the lesion types was 0.837. On the last follow-up MRI scans of 19 patients, the size decreased (median, 5.8 mm; IQR, 3.4–8.5 mm), and the type changed from A or B to C in 11 patients. The lesions resolved in four patients. In five patients who underwent prostatectomy, caseous necrosis on histopathology matched with the non-enhancing components of type B lesions and the entire type C lesions.

Conclusion: BCG-related GP demonstrated three imaging patterns on multiparametric MRI. Contrast-enhanced T1-weighted imaging and DWI may play a role in its differential diagnosis from prostate cancer.

Keywords: *Magnetic resonance imaging; BCG vaccine; Prostatitis; Prostate cancer*

INTRODUCTION

The Bacillus Calmette–Guérin (BCG) vaccine is primarily used against tuberculosis. Since Morales et al. [1] introduced intravesical BCG instillation as a treatment for superficial bladder cancer, BCG immunotherapy for non-muscle invasive bladder cancer after transurethral resection has been widely used [1-3]. It is hypothesized that immune system activation and the induction of inflammatory response after BCG treatment play important roles in treatment [4].

BCG-related granulomatous prostatitis (GP), resulting from contaminated urine reflux from a prostatic urethra, is one of the complications after intravesical BCG instillation. Its incidence is estimated between 0.8% and 3.3% [5-8]. It is usually in the peripheral zone (PZ) because of the obtuse angle between the PZ and the urethra [9-12].

Intravesical BCG instillation is associated with elevated prostate-specific antigen levels in up to 40% of patients [5,13]. Thus, it is important to differentiate BCG-related

Received: November 18, 2020 **Revised:** June 17, 2021
Accepted: June 19, 2021
Corresponding author: Young Taik Oh, MD, PhD, Department of Radiology, Research Institute of Radiological Science, Severance Hospital, Yonsei University College of Medicine, 50-1 Yonsei-ro, Seodaemun-gu, Seoul 03722, Korea.
• E-mail: oytaik@yuhs.ac

Korean Journal of Radiology
KJR

GP from prostate cancer (PCa). There have been several studies on the MRI features of BCG-related GP. The signal intensity (SI) of BCG-related GP on T1-weighted images, T2-weighted images, and diffusion-weighted imaging (DWI) were different [14-20]. On high b-value DWI, the high and low SI are thought to be related to acute and chronic manifestations, respectively [14,16]. The lesions of caseous necrosis showed rim or no enhancement [16,20]. However, these studies were case reports or series for 10 or fewer patients and did not assess the time course.

The purpose of this study was to categorize the multiparametric MRI features of BCG-related GP and discover the manifestations for its differential diagnosis from PCa.

MATERIALS AND METHODS

Study Participants

The Institutional Review Board of our hospital approved this retrospective study, and the need for informed consent was waived (IRB No. 1-2020-0024).

Our hospital database of pathology reports between January 2011 and April 2019 was queried with keywords such as "prostate," "BCG," "granuloma," "granulomatous inflammation," and "caseous necrosis". Eighty-four patients were pathologically diagnosed with BCG-related GP. Among them, 38 underwent MRI between BCG instillation and pathologic diagnosis. Patients without focal lesions on MRI, which would be due to the small lesion size or inactive phase of the disease, were excluded. Finally, 24 male (mean age ± standard deviation, 66.0 ± 9.4 years; range, 50–88 years) with pathologically confirmed BCG-related GP were included (Supplementary Fig. 1). For patients with multiple MRI scans, the last follow-up MRI scan was reviewed to assess the time course. The MRI scans between the first and last were examined for consistency of the lesions. Histologic diagnosis was done using systematic transrectal ultrasound-guided prostate biopsy in 20 patients and radical cystectomy in four patients. Among the 20 patients who underwent core-needle biopsy, five patients with concurrent PCa underwent radical prostatectomy. Clinically significant PCa was characterized by a Gleason score of > 7 on a whole prostate specimen, tumor volume of > 0.5 cc, or extraprostatic extension.

MRI Protocol

Three types of 3T MRI machines (Intera Achieva, Philips Medical System; Discovery MR750, GE Medical Systems; TrioTim, Siemens) were used with a phased-array body coil. Before the MRI, 20 mg of butyl scopolamine (Buscopan; Boehringer Ingelheim) was injected to suppress bowel peristalsis. The MRI sequences included T1-weighted, T2-weighted, contrast-enhanced (CE) T1-weighted imaging, and DWI. The acquisition parameters are summarized in Table 1.

Image Interpretation

Two radiologists (with 18 and 3 years of experience interpreting PCa, respectively) blinded to the clinical and pathologic data independently interpreted the MRI scans. On T2-weighted images, the SI of the lesions was graded on three scales; isointense or moderately hypointense to normal PZ and markedly hypointense similar to obturator internus. The size of the largest lesion was measured on T2-weighted images. On high b-value DWI, the SI of the lesions was compared to the SI of the normal PZ. Thereafter, we interpreted the MRI in consensus and divided the

Table 1. Scan Parameters

	T2-Weighted Sequence	DWI*	T1-Weighted Sequence	T1-Weighted, Contrast-Enhanced Sequence†
Fat saturation	No	Yes	No	Yes
Orientation	Axial	Axial	Axial	Axial or sagittal
Repetition time, msec	3100–6500	3290–5000	450–771	2.7–4.7
Echo time, msec	80–120	56–85	10–14.9	1.4–1.8
Field of view, mm	200–240	200–340	200–240	200–260
Matrix	512 x 360–320 x 224	192 x 192–128 x 80	512 x 353–320 x 224	272 x 268–256 x 128
b-factor, s/mm^2		0 and 1000		
Slice thickness, mm	3–6	3–6	3–6	4–5

*Apparent diffusion coefficient maps were generated from the DWI data using the mono-exponential model, †A bolus injection of contrast agent (Gadoterate meglumine, Dotarem, Guerbet) was administered using a power injector and followed by a 20 mL saline flush. The dose and injection rate of the contrast agent was 0.1 mmoL/kg body weight and 2–3 mL/s, respectively. DWI = diffusion-weighted imaging

https://doi.org/10.3348/kjr.2020.1369

MRI patterns into three types. Sequential changes of the initially dominant lesions were evaluated on the last MRI scans based on consensus.

Imaging Patterns of BCG-Related GP

We categorized the MRI patterns of BCG-related GP. The lesions were classified into three types (A, B, and C) according to the CE T1-weighted imaging and DWI. Figure 1 shows schematic illustrations of the three types. Type A lesions demonstrate diffuse enhancement. Type B lesions have a well-defined non-enhancing component surrounded by an enhancing component. Both type A and B lesions show considerable diffusion restriction. Type C lesions demonstrate poor rim enhancement and low SI on high b-value DWI. Type D was reserved for enhancing lesions without diffusion restriction, which is unlikely to exist. If a patient had multiple lesions, we evaluated the largest dominant lesion.

Histopathological Analysis

Pathological analyses of the radical prostatectomy specimens were performed by a pathologist (9 years of experience for PCa). Briefly, the resected prostate gland specimen was first grossly analyzed, fixed in neutral buffered formalin, and embedded in a paraffin block. Whole-mount step sections were cut transversely at regular intervals from the apex of the prostate to the tips of the seminal vesicles. H&E-stained slides of each section were examined, and the pathologic findings were matched with the MRI findings. In the patients without whole-mount specimens, the result of the systematic prostate biopsy was used to localize BCG-related GP.

Statistical Analysis

We evaluated the inter-reader agreement for the imaging patterns using Cohen's kappa coefficient. Statistical analysis was performed using R software (version 3.5.3.; R Foundation for Statistical Computing).

RESULTS

The full clinical data and MRI features in the 24 individual patients are provided in Supplementary Table 1.

Imaging Features on Initial MRI

The interval between the first day of BCG instillation and the MRI scans ranged from 59 to 451 days (median, 172 days) for the initial MRI and from 243 to 2271 days (median, 891 days) for the last MRI. Of the 24 patients, 7, 15, and 2 patients had type A, B, and C lesions, respectively. The

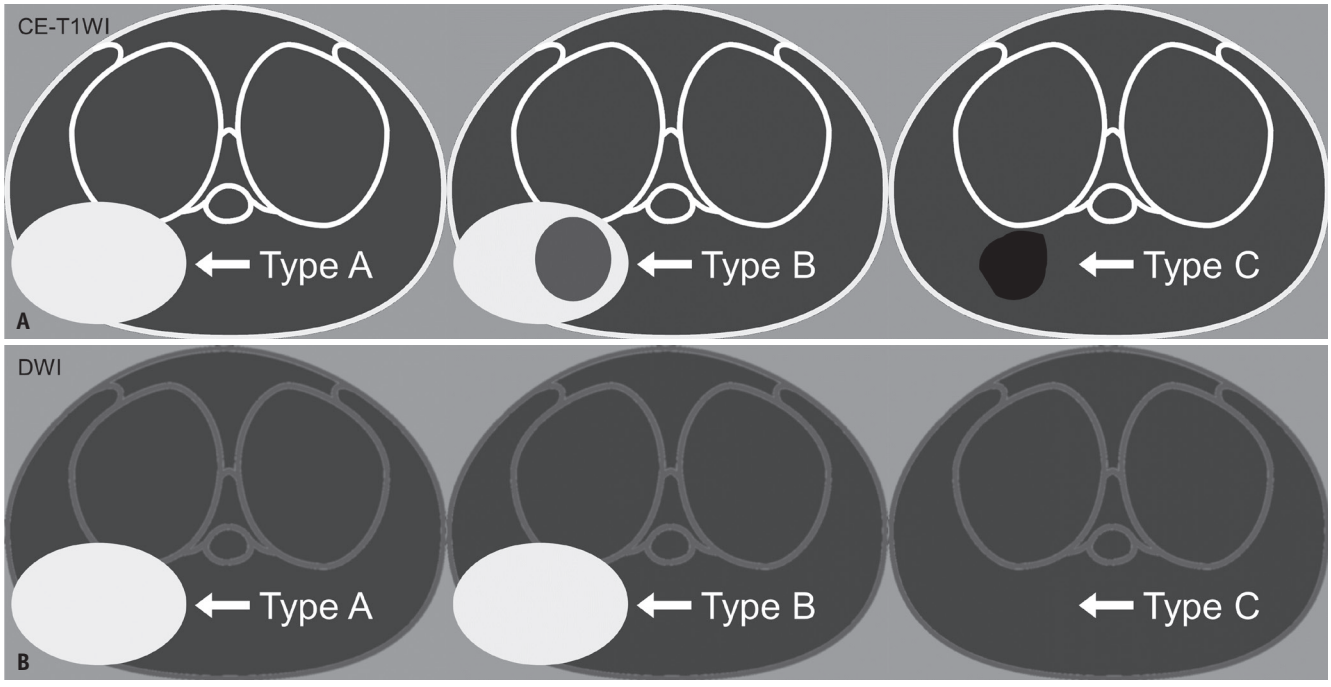

Fig. 1. Schematic illustration of Bacillus Calmette–Guérin-related granulomatous prostatitis types A, B, and C.
A. On contrast-enhanced T1-weighted imaging, a diffusely enhancing lesion is classified as type A. If a non-enhancing area is surrounded by an enhancing component, the lesions are classified as type B. Type C lesions does not enhance. **B.** On high b-value DWI, type A and B lesions demonstrate a high signal intensity on high b-value DWI. Type C lesions are not discernible on DWI. DWI = diffusion-weighted imaging

https://doi.org/10.3348/kjr.2020.1369

Korean Journal of Radiology
KJR

Table 2. Multiparametric Features on the Initial MRI of Bacillus Calmette–Guérin-Related Granulomatous Prostatitis Categorized by Type A, B, and C

	Type A	Type B	Type C
Margin	Smooth	Smooth	Angled or distorted
T2WI	Variable	Variable	Markedly low
CE-T1WI*	Diffuse enhancement	Inner poorly enhancing component	No
High b-value DWI*	High	High	Low
ADC	Low	Low	Low

*Key series for the proposed imaging pattern. ADC = apparent diffusion coefficient, CE = contrast-enhanced, DWI = diffusion-weighted image, T1WI = T1-weighted image, T2WI = T2-weighted image

multiparametric MRI features are detailed in Table 2. On T2-weighted images, SI was moderately hypointense relative to PZ in 22 patients with type A and B lesions. Type C lesions in two patients were markedly hypointense. On the ADC map, all the lesions showed low values. The median diameter of the GP was 22 mm (IQR, 18–26 mm).

Comparison of Initial and Last Follow-Up MRI

Follow-up MRI was performed for 19 patients. Five patients were treated with tuberculosis medications between the MRI scans. The imaging pattern was changed in 12 patients, and the lesions were resolved in 4 patients. Of the six type A patients, the type was changed to B in one and C in three. The lesions of the two remaining type A patients were resolved. Of the 12 type B patients, the lesions did not change in two patients, changed to C in eight patients, and disappeared in two patients. The only follow-up type C lesion was unchanged. The SI decreased on high b-value DWI when the types changed from A or B to C (Fig. 2). The type C lesions that changed from type A or B showed a polygonal shape with notches. The size was decreased in 18 of the 19 patients (median, 22 to 6 mm).

Patients with Concurrent PCa

Five patients underwent prostatectomy for concurrent PCa. The PCa in four patients was clinically significant and demonstrated homogeneous enhancement, which is the same as type A. The clinically significant PCa was in a transition zone in three patients and the PZ in one patient. The cancer and BCG-related GP lesions were in separate locations.

The BCG-related GP was type B and C in two and three patients, respectively. In the two patients with type B lesions (patients no. 11, 19), the caseous necrosis on histopathology matched with the poorly enhancing areas. The enhancing areas surrounding the caseous necrosis represented active inflammation. Both enhancing and non-enhancing components of the type B lesions showed diffusion restriction (Fig. 3). In the three patients with type C lesions (patients no. 1, 4, 12), the caseous necrosis on histopathology matched with the entire extent of lesions that demonstrated a poor enhancement and low SI on high b-value DWI (Fig. 3, Supplementary Fig. 2).

Inter-Reader Agreement for Imaging Pattern

Table 3 is a cross-tabulation for the lesion classifications by each reader. Cohen's kappa value was 0.837.

DISCUSSION

We propose the MRI imaging patterns in BCG-related GP based on sequential changes and histologic findings. The strong inter-reader agreement (kappa = 0.837) observed in this study may provide proof of the simplicity and clarity of these imaging patterns. In previous studies on MRI features in BCG-related GP [14-20], the number of patients was limited. We analyzed 24 patients and, to the best of our knowledge, this study has the largest group of patients with pathologically confirmed BCG-related GP. Follow-up MRI scans of 19 patients were compared with the initial MRI scans to analyze sequential changes.

Gottlieb et al. [14] proposed two patterns for the acute and chronic phases of BCG-related GP based on DWI. We used DWI and CE T1-weighted imaging findings to guide the diagnoses. Types A and B are regarded as acute stages, which show diffusion restriction on DWI and intense enhancement. The difference is the absence and presence of a well-defined poorly enhancing area in types A and B, respectively. Type C is a chronic lesion showing poor enhancement and a low SI on high b-value DWI.

PCa can mimic or overlap with BCG-related GP; therefore, we need to differentiate them using MRI findings. Type C lesions are scored 1 by Prostate Imaging-Reporting and Data System v2.1 due to their low SI on high b-value DWI.

 https://doi.org/10.3348/kjr.2020.1369

In addition, Suzuki et al. [18] proposed the polygonal shape of the nodule with a notch, and a markedly low SI on T2-weighted images helps differentiate GP from PCa. For type B lesions, CE T1-weighted imaging plays a role in the differential diagnosis of BCG-related GP from PCa. Type B lesions demonstrate a well-defined poorly enhancing portion

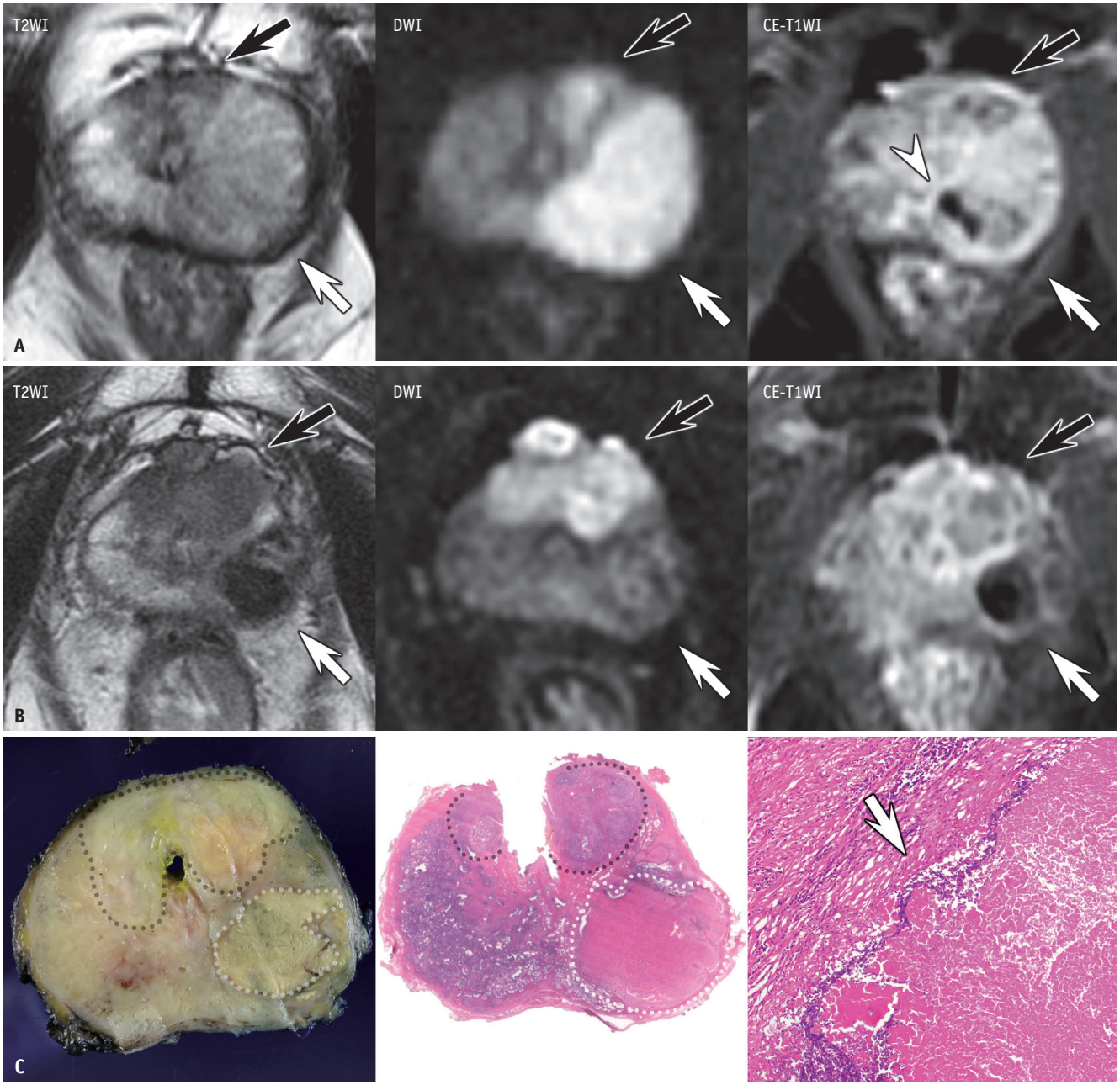

Fig. 2. Images of a 61-year-old male (patient no. 1) with concurrent prostate cancer (black arrows) and granulomatous prostatitis (arrows).
A. Initial MRI was taken 59 days after intravesical Bacillus Calmette–Guérin therapy. Prostate-specific antigen level: 5.12 ng/mL. T2WI shows a heterogeneously decreased signal intensity in the enlarged left peripheral zone. The increased signal intensity on high b-value DWI and enhancement on the CE-T1WI suggest an acute phase of the disease. The intralesional area (arrowhead) with poor enhancement indicates a type B imaging pattern. **B.** Follow-up MRI was performed 6 years later to find the cause of serum prostate-specific antigen elevation (28.5 ng/mL). T2WI shows a decrease in size, distorted margins, and signal intensity as low as that of the obturator internus. The granulomatous prostatitis is now classified as type C due to decreased signal intensity on high b-value DWI and poor enhancement on CE-T1WI. Note the growth of prostate cancer in the anterior transition zone, which was missed on the initial MRI scan. The prostate cancer was hypointense on T2WI, diffusion restrictive, and heterogeneously enhanced. **C.** Histologic specimen reveals caseous necrosis (white dots and arrow). Concurrent prostate cancer (black dots) is observed in the anterior prostate (hematoxylin-eosin stain; original magnificant, x 1, x 100). CE = contrast-enhanced, DWI = diffusion-weighted imaging, T1WI = T1-weighted image, T2WI = T2-weighted image

https://doi.org/10.3348/kjr.2020.1369

Korean Journal of Radiology
KJR

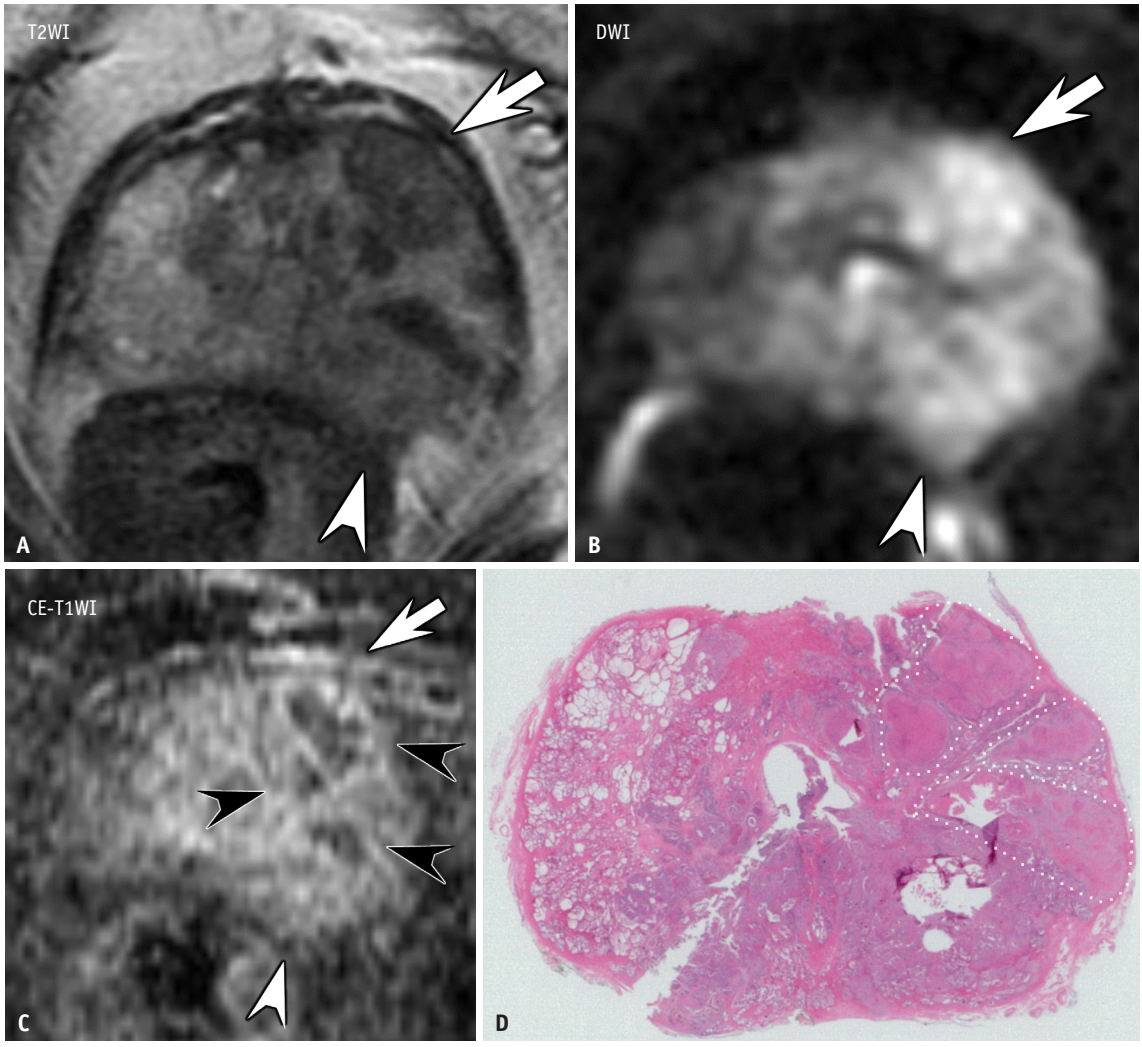

Fig. 3. Granulomatous prostatitis (arrows in A-C) with extraprostatic extension (arrowheads in A-C) in a 67-year-old male (patient no. 19) treated with Bacillus Calmette–Guérin instillation 255 days earlier (prostate-specific antigen level: 4.56 ng/mL).
A. On T2WI, the lesion is heterogeneously hypointense. **B.** On high b-value DWI, the lesion shows increased signal intensity. **C.** On CE T1WI, the lesion shows heterogeneous enhancement. **D.** Histologic specimen reveals caseous necrosis (white dots) corresponding to areas of poor enhancement on MRI (black arrowheads, **C**) (hematoxylin-eosin stain; original magnification, x 1). CE = contrast-enhanced, DWI = diffusion-weighted imaging, T1WI = T1-weighted image, T2WI = T2-weighted image

that corresponds to the caseous necrosis, which is unlikely to present in PCa. In our study, the type B lesions of the four patients with clinically significant PCa showed poorly enhancing areas, in contrast to the diffuse enhancement of concurrent PCa.

The differential diagnoses of type A lesions are more challenging. Identifying a decrease in size and a change of the type on follow-up imaging may be crucial for excluding PCa without biopsy. For diagnosis based on initial MRI, a clue for diagnosis may be the different enhancement kinetics on dynamic CE (DCE)-MRI. Uysal et al. [21] reported the diagnostic potential of DCE-MRI using the low time to peak of PCa and the high time to peak of prostatitis. However, Dianat et al. [19] reported a case of BCG-related GP that showed early enhancement and washout. Moreover, the early enhancement and washout kinetics of PCa is not evident in some patients [22]. Hence, more dedicated research on enhancement kinetics is required. The decrease in size and change in the type on follow-up imaging. Follow-up imaging may be very crucial by identifying a decrease in size or disappearance.

This study has several potential limitations. First, the MRI protocols were heterogeneous. The MRI scans were obtained from various machines with heterogeneous protocols. Due to the heterogeneity of protocols, quantitative analysis was not available. Second, the date intervals for follow-up

 https://doi.org/10.3348/kjr.2020.1369

Table 3. Inter-Reader Agreement in Interpreting the MRI Pattern in Bacillus Calmette–Guérin-Related Granulomatous Prostatitis

	Reader			
	Type A	Type B	Type C	Total
Reader				
Type A	7			7
Type B		15	1	16
Type C			1	1
Total	7	15	2	24

Cohen's kappa value = 0.837.

MRI acquisition varied largely. The considerable variation made it difficult to correlate the duration and stage of the disease. Third, there may be bias due to the limited diagnostic performance of core-needle biopsy. The imaging features were evaluated in prostate zones with concordant results on biopsy. However, there is still the risk of false-negatives based on the extent of the disease. Fourth, this retrospective study involved only a few patients to draw a clinical implication. A prospective multicenter study of a larger group of patients is needed to show external validity and clinical guidance.

We propose three MRI patterns for BCG-related GP based on histologic findings and sequential changes. Contrast-enhanced T1-weighted imaging and DWI may play a role in the differential diagnosis of type B and C lesions from PCa. Monitoring followed by biopsy is recommended for patients with type A lesions.

Supplement

The Supplement is available with this article at https://doi.org/10.3348/kjr.2020.1369.

Conflicts of Interest

The authors have no potential conflicts of interest to disclose.

Author Contributions

Conceptualization: Young Taik Oh. Data curation: Young Taik Oh, Seungsoo Lee. Formal analysis: Young Taik Oh, Seungsoo Lee. Investigation: Young Taik Oh, Seungsoo Lee, Hye Min Kim. Methodology: Young Taik Oh, Seungsoo Lee, Hye Min Kim. Project administration: Young Taik Oh. Resources: Young Taik Oh, Hye Min Kim. Software: Seungsoo Lee. Supervision: Young Taik Oh. Validation: Dae Chul Jung, Hyesuk Hong. Visualization: Seungsoo Lee, Hye Min Kim. Writing—original draft: Seungsoo Lee. Writing—review & editing: Young Taik Oh, Dae Chul Jung, Hyesuk Hong.

ORCID iDs

Seungsoo Lee
https://orcid.org/0000-0002-6268-575X
Young Taik Oh
https://orcid.org/0000-0002-4438-8890
Hye Min Kim
https://orcid.org/0000-0002-2899-9480
Dae Chul Jung
https://orcid.org/0000-0001-5769-5083
Hyesuk Hong
https://orcid.org/0000-0001-7398-2517

Funding Statement

None

REFERENCES

1. Morales A, Eidinger D, Bruce AW. Intracavitary Bacillus Calmette-Guerin in the treatment of superficial bladder tumors. *J Urol* 2017;197:S142-S145
2. Babjuk M, Böhle A, Burger M, Capoun O, Cohen D, Compérat EM, et al. EAU guidelines on non–muscle-invasive urothelial carcinoma of the bladder: update 2016. *Eur Urol* 2017;71:447-461
3. Spiess PE, Agarwal N, Bangs R, Boorjian SA, Buyyounouski MK, Clark PE, et al. Bladder cancer, version 5.2017, NCCN Clinical Practice Guidelines in Oncology. *J Natl Compr Canc Netw* 2017;15:1240-1267
4. Donin NM, Lenis AT, Holden S, Drakaki A, Pantuck A, Belldegrun A, et al. Immunotherapy for the treatment of urothelial carcinoma. *J Urol* 2017;197:14-22
5. Leibovici D, Zisman A, Chen-Levyi Z, Cypele H, Siegel YI, Faitelovich S, et al. Elevated prostate specific antigen serum levels after intravesical instillation of bacillus Calmette-Guerin. *J Urol* 2000;164:1546-1549
6. Alexander RB, Mann DL, Borkowski AA, Fernandez-Vina M, Klyushnenkova EN, Kodak J, et al. Granulomatous prostatitis linked to HLA-DRB1*1501. *J Urol* 2004;171:2326-2329
7. Lamm DL, van der Meijden PM, Morales A, Brosman SA, Catalona WJ, Herr HW, et al. Incidence and treatment of complications of bacillus Calmette-Guerin intravesical therapy in superficial bladder cancer. *J Urol* 1992;147:596-600
8. Stillwell TJ, Engen DE, Farrow GM. The clinical spectrum of granulomatous prostatitis: a report of 200 cases. *J Urol* 1987;138:320-323
9. Butel R, Ball R. The distribution of BCG prostatitis: a clue for pathogenetic processes? *Prostate* 2018;78:1134-1139
10. LaFontaine PD, Middleman BR, Graham SD Jr, Sanders WH.

Incidence of granulomatous prostatitis and acid-fast bacilli after intravesical BCG therapy. *Urology* 1997;49:363-366
11. García Solano J, Sánchez Sánchez C, Montalbán Romero S, Pérez-Guillermo M. Diagnostic dilemmas in the interpretation of fine-needle aspirates of granulomatous prostatitis. *Diagn Cytopathol* 1998;18:215-221
12. Uzoh CC, Uff JS, Okeke AA. Granulomatous prostatitis. *BJU Int* 2007;99:510-512
13. Beltrami P, Ruggera L, Cazzoletti L, Schiavone D, Zattoni F. Are prostate biopsies mandatory in patients with prostate-specific antigen increase during intravesical immuno- or chemotherapy for superficial bladder cancer? *Prostate* 2008;68:1241-1247
14. Gottlieb J, Princenthal R, Cohen MI. Multi-parametric MRI findings of granulomatous prostatitis developing after intravesical bacillus calmette-guérin therapy. *Abdom Radiol (NY)* 2017;42:1963-1967
15. Kim CY, Lee SW, Choi SH, Son SH, Jung JH, Lee CH, et al. Granulomatous prostatitis after intravesical Bacillus Calmette-Guérin instillation therapy: a potential cause of incidental F-18 FDG uptake in the prostate gland on F-18 FDG PET/CT in patients with bladder cancer. *Nucl Med Mol Imaging* 2016;50:31-37
16. Bour L, Schull A, Delongchamps NB, Beuvon F, Muradyan N, Legmann P, et al. Multiparametric MRI features of granulomatous prostatitis and tubercular prostate abscess. *Diagn Interv Imaging* 2013;94:84-90
17. Ma W, Kang SK, Hricak H, Gerst SR, Zhang J. Imaging appearance of granulomatous disease after intravesical Bacille Calmette-Guerin (BCG) treatment of bladder carcinoma. *AJR Am J Roentgenol* 2009;192:1494-1500
18. Suzuki T, Takeuchi M, Naiki T, Kawai N, Kohri K, Hara M, et al. MRI findings of granulomatous prostatitis developing after intravesical Bacillus Calmette-Guérin therapy. *Clin Radiol* 2013;68:595-599
19. Dianat SS, Matoso A, Carter BH, Macura KJ. Multiparametric MRI findings of granulomatous prostatitis after intravesical bacillus Calmette-Guérin therapy in a patient undergoing active surveillance. *Clin Genitourin Cancer* 2014;12:e215-e219
20. Diaz de Leon A, Costa DN, Francis F, Pedrosa I. Case 258: granulomatous prostatitis. *Radiology* 2018;289:267-271
21. Uysal A, Karaosmanoğlu AD, Karcaaltıncaba M, Akata D, Akdogan B, Baydar DE, et al. Prostatitis, the great mimicker of prostate cancer: can we differentiate them quantitatively with multiparametric MRI? *AJR Am J Roentgenol* 2020;215:1104-1112
22. Turkbey B, Rosenkrantz AB, Haider MA, Padhani AR, Villeirs G, Macura KJ, et al. Prostate imaging reporting and data system version 2.1: 2019 update of prostate imaging reporting and data system version 2. *Eur Urol* 2019;76:340-351

 https://doi.org/10.3348/kjr.2020.1369